http://dx.doi.org/10.5012/bkcs.2012.33.2.398

Synthesis and Characterization of SiO_2-Sheathed ZnSe Nanowires

Hyunsu Kim, Changhyun Jin, Soyeon An, and Chongmu Lee*

*Department of Materials science and Engineering, Inha University, Incheon 402-751, Korea. *E-mail: cmlee@inha.ac.kr*
Received October 20, 2011, Accepted November 23, 2011

$ZnSe/SiO_2$ coaxial nanowires were synthesized by a two-step process: thermal evaporation of ZnSe powders and sputter-deposition of SiO_2. Two different types of nanowires are observed: thin rod-like ones with a few to a few tens of nanometers in diameter and up to a few hundred of micrometers in length and wide belt-like ones with a few micrometers in width. Room-temperature photoluminescence (PL) measurement showed that $ZnSe/SiO_2$ coaxial nanowires had an orange emission band centered at approximately 610 nm. The intensity of the orange emission from the SiO_2-sheathed ZnSe nanowires was enhanced significantly by annealing in a reducing atmosphere whereas it was degraded by annealing in an oxidizing atmosphere. The origins of the PL changes by annealing are discussed based on the energy-dispersive X-ray spectroscopy analysis results.

Key Words : Nanostructures, Luminescence, Scanning electron microscopy (SEM), Transmission electron microscopy (TEM), X-ray diffraction

Introduction

It is essential to passivate one-dimensional (1D) nanostructures with insulating materials to avoid crosstalking between the building blocks of complex nanoscale circuits as well as to protect them from contamination and oxidation.[1,2] Passivation also offers many advantages such as substantial reduction of surface states, prevention of the surface from adsorption of unwanted species, prevention of unnecessary charge injection, and partial screening of the external fields.[3,4] In particular, passivation of nanowires is required in fabrication of field effect transistors and sensor devices based on nanowires. Various techniques have been reported to be used to form passivation layers on the 1D nanowire cores. These techniques include sol-gel processes, thermal heating, solution-based methods, chemical vapor deposition, atomic layer deposition, and sputtering.[5-13] On the other hand, silicon dioxide (SiO_2) is known as one of the most suitable insulating material for nanowire passivation owing to its excellent insulating property, low dielectric constant, and high mechanical strength as well as compatibility with other materials widely used in integrated circuits (IC) fabrication. SiO_2 is also optically transparent for light absorption or emission of semiconductor nanowires, resulting in minimal destruction of their intrinsic optical properties such as photoluminescence.[14,15]

Zinc selenide (ZnSe) is an important wide direct band gap compound semiconductor which has attracted significant interest for their potential applications in optoelectronics and electronics. ZnSe is particularly suitable for short-wavelength optoelectronic device applications including blue-green laser diodes[16] and tunable mid-IR laser sources for remote sensing.[17] Recently one-dimensional (1D) nanostructures of ZnSe such as nanowires, nanorods, nanobelts, nanoribbons, nanoneedles, have been synthesized using various techniques including metal-organic chemical vapor deposition (MOCVD),[18] molecular beam epitaxy (MBE)[19] pulsed lased deposition (PLD),[20] and atomic layer deposition (ALD),[21] and thermal evaporation.[22] Among these techniques thermal evaporation may be the simplest one. In this paper, we report the synthesis, structure, and photoluminescence (PL) properties of SiO_2-sheathed ZnSe nanowires. The $ZnSe/SiO_2$ coaxial nanowires were prepared by using a two-step process: thermal evaporation of ZnSe powders on Al_2O_3 substrates and sputtering of SiO_2.

Experimental

We prepared $ZnSe/SiO_2$ coaxial nanowires on Al_2O_3 (0001) substrates. Firstly, ZnSe nanowires were synthesized on 3 nm thick gold (Au) layer-coated c-plane sapphire (Al_2O_3 (0001)) substrates by thermal evaporation of ZnSe powders. The schematic of the heating furnace used for this thermal evaporation process is shown elsewhere.[22] A quartz tube was mounted inside a horizontal tube furnace. The quartz tube consists of two temperature zones: zone A at 850 °C and zone B at 750 °C. An alumina boat loaded with pure ZnSe powders was located in zone A and the Au-coated Al_2O_3 substrate was in zone B. The nitrogen (N_2) gas flow rate was 150 standard cubic centimeters per minute (sccm) and the chamber pressure was 0.5 Torr. The synthesis was performed for 1 h.

Next, coating of the ZnSe nanowires with SiO_2 was carried out by sputtering. The sputter-deposition was carried out at room temperature for 25 min using a 99.999% SiO_2 target in a radio-frequency (rf) magnetron sputtering system. After the vacuum chamber was evacuated to 1×10^{-6} Torr using a turbomolecular pump backed by a rotary pump Ar was supplied at a flow rate of 30 sccm. The system pressure and the rf sputtering power were 2×10^{-2} Torr and 100 W, respectively. Some of the prepared SiO_2-coated ZnSe nanowire samples were subsequently annealed in an O_2 or N_2/3-

mol % H_2 atmosphere at 600 °C for 30 min to see the influence of annealing on the photoluminescence (PL) properties of the coaxial nanowire structures.

The samples were then characterized by using glancing angle (0.5°) X-ray diffraction (XRD, X'pert MPD-Philips with Cu-K_α radiation), scanning electron microscopy (SEM, Hitachi S-4200), transmission electron microscopy (TEM, Phillips CM-200 equipped with an EDX spectrometer). The compositions across the diameter of the 1D coaxial nanostructure samples annealed in different atmospheres were investigated by using the energy-dispersive X-ray spectroscope (EDXS) installed in the TEM. The high resolution TEM (HRTEM) images and the selected area electron diffraction (SAED) patterns were also taken on the same systems. The PL measurements were performed at room temperature by using a He-Cd laser (325 nm) as the excitation source.

Results and Discussion

The SEM image of the as-synthesized SiO_2-sheathed ZnSe nanowires is shown in Figure 1. Two different types of nanowires are observed: thin rod-like ones and wide belt-like ones. The former was a few to a few tens of nanometers in diameter and up to a few hundred of micrometers in length whereas the latter was a few micrometers in width. The enlarged SEM image in the inset clearly shows that a spherical droplet or particle does exist at the tip of a typical rod-like nanowire, which suggests that the ZnSe nanowires have grown through a catalyst-assisted vapor-liquid-solid (VLS) mechanism. The growth mechanism of 1D nanostructures can differ for different process parameters. Particularly, it depends on the growth temperature. The VLS mechanism through which 1D nanostructures grow with an assistance of catalysts is dominant at lower temperatures because thermal energy is not enough for the nucleation and growth of the structure. In contrast, the vapor-solid (VS) mechanism is dominant at higher temperatures where sufficient thermal energy is provided. Close examination of the SEM image the particles exist not only at the end of wires but also other regions. EDX spectra (Figures 2(a) and 2(b)) indicates that chemical composition of the particles (Figure 2(a)) is more or less the same as that of the nanowires (Figure 2(b)). Therefore, we assume that the particles would not influence the PL behavior of the nanowires.

The XRD pattern of SiO_2-sheathed ZnSe nanowires is

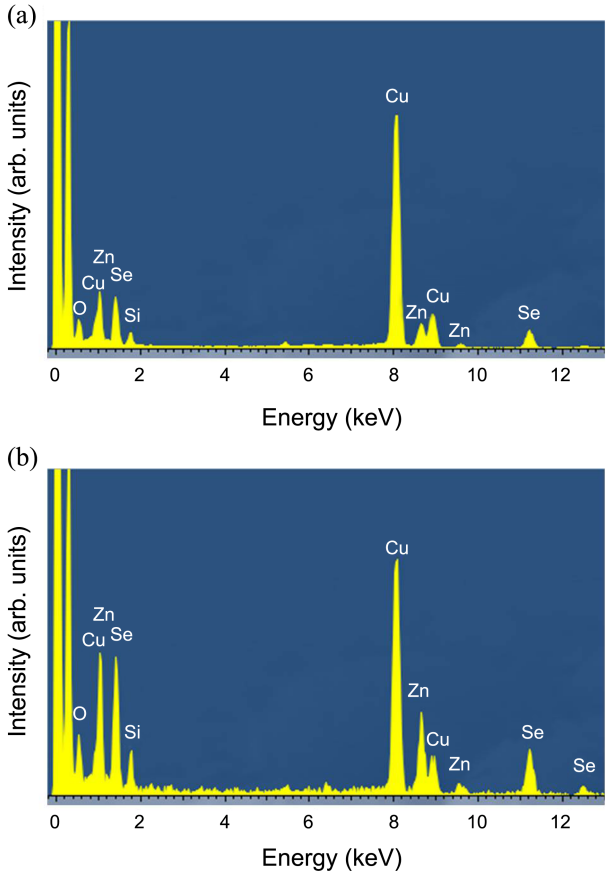

Figure 2. EDX spectra taken from (a) spherical particles and (b) nanowires in Figure 1.

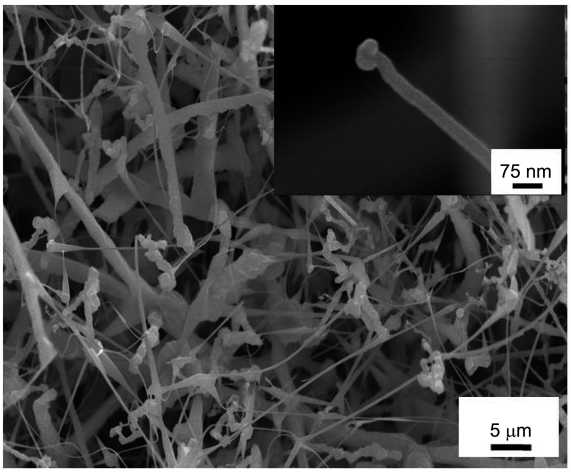

Figure 1. SEM images of SiO_2-sheathed ZnSe nanowires. Two different types of nanowires are observed: thin rod-like ones and wide belt-like ones.

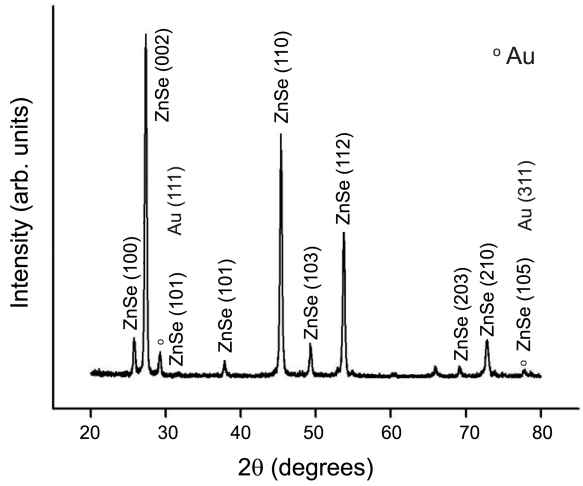

Figure 3. XRD patterns of SiO_2-sheathed ZnSe nanowires prepared by a two-step process: thermal evaporation of ZnSe powders at 600 °C and rf magnetron sputtering of SiO_2 at 100 W for 1 hr.

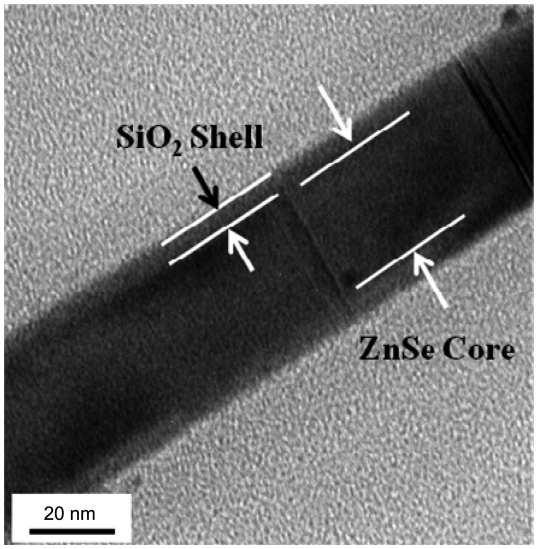

Figure 4. Low-magnification TEM image of a typical SiO_2-sheathed ZnSe nanowires.

shown in Figure 3. All the diffraction peaks in the XRD patterns of SiO_2-sheathed ZnSe nanowires belong to crystalline ZnSe with a simple hexagonal structure (JCPDS card NO. 15-0105). No appreciable diffraction peak of SiO_2 was found, indicating that it is amorphous. No diffraction peaks of elemental Zn, Se, Si, and any other contaminants except Au, which used as a catalyst, were observed, suggesting that the nanowires are very pure.

Figure 4 presents the low-magnification TEM image of a typical as-synthesized (unannealed) SiO_2-sheathed ZnSe nanowire. The TEM image of the nanowire clearly showed a rod-like core (a dark area inside) and a shell (the less dark areas on both edge sides of the dark area) with a high thickness uniformity along the length of the nanowire. The thicknesses of the ZnSe core and the SiO_2 shell layer were about ~350 and ~60 nm, respectively. The fringe on the upper right side of the local high resolution TEM (HRTEM) image in Figure 5(a) clearly indicates that the ZnSe core is monocrystalline. In contrast, no fringe pattern was observed on the lower left side, confirming that the SiO_2 shells are amorphous.

The associated SAED pattern (Figure 5(b)) shows a set of simple hexagonal electron diffraction pattern spots corresponding to the ZnSe core. This result is consistent with the XRD pattern of the ZnSe-core/SiO_2-shell nanowires in Figure 3. The resolved distance between two neighboring fringes shown in Figure 5(a) is 0.343 nm, which is in good agreement with the interplanar spacing of the {100} lattice plane family of simple hexagonal ZnSe with lattice parameters of a = 0.3996 nm and c = 0.655 nm (JCPDS 15-0105).

The room temperature PL spectrum of ZnSe nanostructures is known to be typically dominated by two characteristic emission bands:[23-28] (1) a near-band edge (NBE) emission band centered at around 465 nm and (2) a broad deep level emission band in the wavelength range of 500-680 nm. The NBE emission is known to originate from

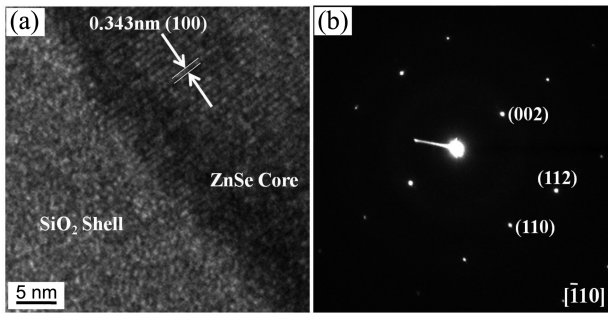

Figure 5. (a) High-magnification TEM image and (b) corresponding SAED pattern of a typical SiO_2-sheathed ZnSe nanowires.

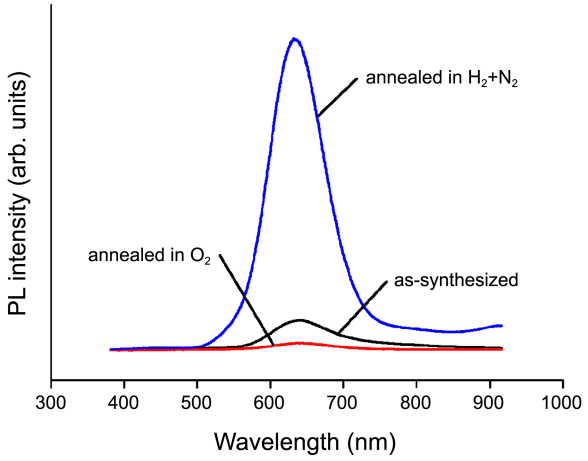

Figure 6. Photoluminescence spectra of the as-synthesized SiO_2-sheathed ZnSe nanowires, those annealed at 600 °C in an N_2/3mol %-H_2 atmosphere, and those annealed at 600 °C in an O_2 atmosphere.

bound excitons whereas the deep level emission is mainly attributed to deep levels such as vacancies, interstitials, and surface states.[23-27] The PL spectra of the SiO_2-sheathed ZnSe nanowire samples annealed in O_2 and N_2/3-mol % H_2 atmospheres are displayed in Figure 6 along with that of the as-synthesized one. The PL spectra of the as-synthesized nanowire samples were dominated by a broad deep level-related orange emission band centered at around 610 nm and the NBE emission was negligible. The emission at ~610 nm does not appear to be from the SiO_2 shell but from the ZnSe core since no emission band of SiO_2 nanostructures has been reported at the wavelength of ~610 nm. The SiO_2 nanostructures were reported to have two PL emission bands: one centered in the range of 414-470 nm[29-32] and the other at around 540 nm.[33] As can be seen in Figure 6, the deep level-related emission from the SiO_2-sheathed ZnSe nanowires depended on the annealing atmosphere strongly. The intensity of the orange emission from the sheathed nanowire sample annealed in a N_2/H_2 atmosphere was by far higher than that of the orange emission from the as-synthesized one, whereas the intensity of the orange emission from those annealed in an O_2 atmosphere was lower than that of the orange emission from the as-synthesized one.

We performed EDXS analyses to investigate the origin of

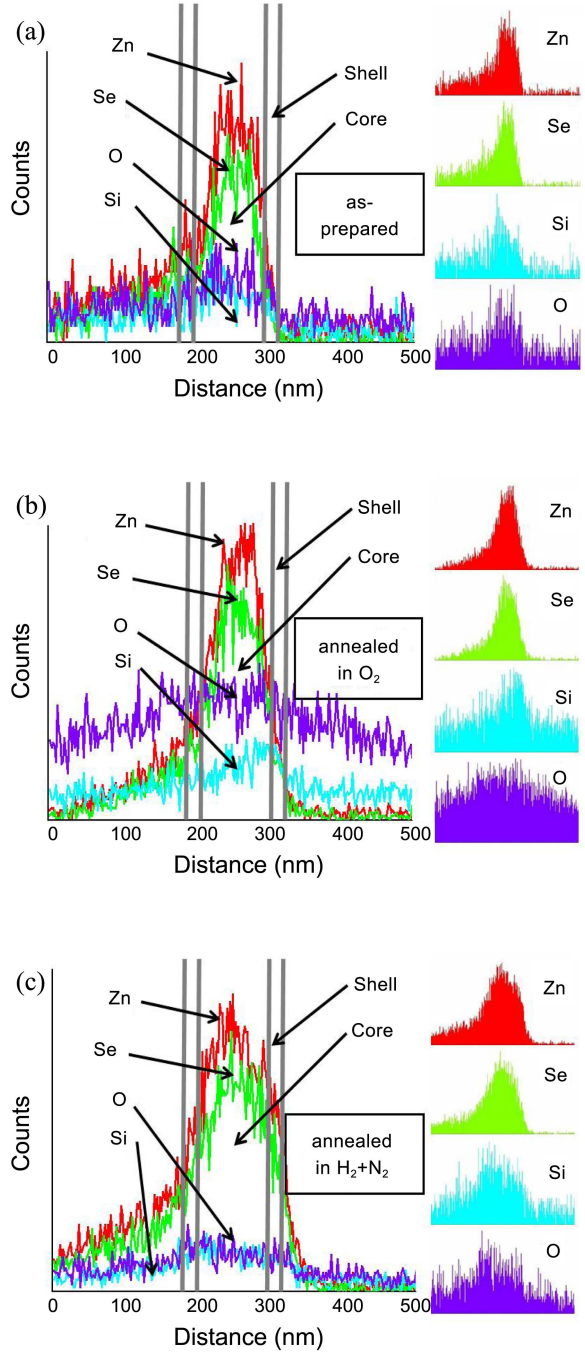

Figure 7. EDXS line scanning concentration profiles of a typical SiO_2-sheathed ZnSe nanowire: (a) as-synthesized, (b) O_2-annealed, and (c) N_2/H_2-annealed.

the enhancement in the PL property of the sheathed nanowires by annealing in a reducing atmosphere. Figure 7(a) shows the EDXS concentration profiles of Zn, Se, Si, and O along the diameter of a typical sheathed nanowire. One should be cautious in interpreting these profiles. In Figures 7(a), 7(b) and 7(c), it looks as if Si atoms existed not only in the shell regions but also in the core regions. Nevertheless, it is not true but due to the overlapping of the core and shell layers. The Si concentration profile in the core region in each of Figures 7(a)-(c) is actually the sum of the Si concentrations in the front-side SiO_2 shell layer, the backside SiO_2 shell layer, and the ZnSe core because X-ray beam simultaneously scans all those three layers overlapped in the beam direction.

A comparison of the Zn and Se profiles with the Si and O profiles reveals that Zn and Se elements concentrate in the core region while Si and O elements concentrate in the shell region. This concentration profiles are in good agreement with what can be expected for the ZnSe-core/SiO_2-shell nanowires. The Zn concentration is somewhat higher than the Se concentration in the core region of a typical as-synthesized nanowire (Figure 7(a)), suggesting that there have already existed high concentrations of Zn interstitials and Se vacancies in the ZnSe cores before annealing, which is in good agreement with previous reports.[23-27] A close examination of the concentration profiles indicates that the concentration of O in the core region after annealing in a N_2/3-mol % H_2 atmosphere (Figure 7(c)) is much lower than that before annealing in a N_2/3-mol % H_2 atmosphere (Figure 7(a)). This suggests that the hydrogen atoms flowed into the cores during annealing in an N_2/H_2 atmosphere have removed some of the O atoms from the cores by reacting with them. If hydrogen atoms flow into the cores during annealing in an N_2/H_2 atmosphere, the reaction between H_2 molecules and Se atoms will also occur besides the reaction between H_2 molecules and O atoms. In other words, some of the Zn-Se bonds will be broken to form H-Se bonds because the strength of the H-Se bond is larger than that of the Zn-Se bond (E_{Se-H} = 73 Kcal/mol, E_{Se-Zn} = 32.6 Kcal/mol).[34] As a result of this reaction, either Zn interstitials or Se vacancies will newly form in the cores. Consequently, the concentration of Zn interstitials and Se vacancies are increased by annealing in a reducing atmosphere and the orange emission is, in turn, enhanced by the increase in deep level concentration.

In contrast, the degradation in the orange emission by annealing in an oxidizing atmosphere might be explained in the opposite way. The concentration of O in the core region is much higher after annealing in an O_2 atmosphere (Figure 7(b)) than that before annealing in an O_2 atmosphere (Figure 7(a)). We surmize that Zn atoms in the interstitial sites make bonds with the O atoms flowed into the core region during the annealing process, resulting in a decrease in the concentration of Zn interstitials in the cores. On the other hand, some of the O atoms flowed into the core region remove the Se vacancies by occupying the vacant sites, resulting in a decrease in the concentration of Se vacancies. Consequently, the concentrations of both Zn interstitials and Se vacancies are decreased by annealing in an oxidizing atmosphere and the orange emission is, in turn, depressed by the decrease in the deep level concentration.

Summary and Conclusions

We have fabricated ZnSe-core/SiO_2-shell 1D nanostructures by using a two-step process consisting of thermal evaporation of ZnSe powders and sputtering of Si in an O_2

atmosphere. The ZnSe-cores of the as-prepared nanowires were of a single crystal nature with a simple hexagonal structure while the SiO_2-shells were amorphous. The PL spectra of the as-synthesized nanowire samples were dominated by a broad deep level-related orange emission band centered at around 610 nm and the NBE emission was negligible. The deep level-related emission of the SiO_2-sheathed ZnSe nanowires strongly depended on the annealing atmosphere. The orange emission of the sheathed nanowire sample annealed in a N_2/H_2 atmosphere was by far higher in intensity than that of the unannealed one, whereas the orange emission of those annealed in an O_2 atmosphere was lower in intensity than that of the unannealed one. If hydrogen atoms flow into the cores during annealing in an N_2/H_2 atmosphere, some of the Zn-Se bonds will be broken to form H-Se bonds because the strength of the Se-H bond is larger than that of the Zn-Se bond. As a result of these reactions, either Zn interstitials or Se vacancies will newly form in the cores. Consequently, the concentration of Zn interstitials and Se vacancies are increased by annealing in a reducing atmosphere and the orange emission is, in turn, enhanced by the increase in deep level concentration. In contrast, the degradation of the orange emission by annealing in an oxidizing atmosphere can be explained in the opposite way. Zn atoms in the interstitial sites make bonds with the O atoms flowed into the core region during the annealing process, resulting in a decrease in the concentration of Zn interstitials in the cores. On the other hand, some of the O atoms flowed into the core region remove the Se vacancies by occupying the vacant sites, resulting in a decrease in the concentration of Se vacancies.

Acknowledgments. This work was supported by the Korean Research Foundation through 'the 2007 National Research Lab. Program'.

References

1. Lauhon, L. J.; Gudiksen, M. S.; Wang, D.; Lieber, C. M. *Nature* **2002**, *420*, 57.
2. Morales, A. M.; Lieber, C. M. *Science* **1998**, *279*, 208.
3. Li, B.; Bando, Y.; Goldberg, D.; Uemura, Y. *Appl. Phys. Lett.* **2003**, *83*, 3999.
4. Liang, X.; Tan, S.; Tang Z.; Kotov, N. A. *Langmuir* **2004**, *20*, 1016.
5. Kim, N. H.; Kim, H. W.; Seoul, C.; Lee, C. *Mater. Sci. Eng. B* **2004**, *111*, 131.
6. Park, S.; Kim, H.; Lee, J. W.; Kim, H. W.; Lee, C. *J. Kor. Phys. Soc.* **2008**, *53*, 657.
7. Jun, J.; Jin, C.; Kim, H.; Kang, J.; Lee, C. *Appl. Phys. A* **2009**, *96*, 813.
8. Park, S.; Jun, J.; Kim, H. W.; Lee, C. *Solid State Comm.* **2009**, *149*, 315.
9. Jun, J.; Jin, C.; Kim, H.; Park, S.; Lee, C. *Appl. Surf. Sci.* **2009**, *255*, 8544.
10. Jin, C.; Kim, H.; Kim, H. W.; Lee, C. *J. Luminescence* **2010**, *130*, 516.
11. Jin, C.; Kim, H.; Baek, K.; Kim, H. W.; Lee, C. *Cryst. Res. Technol.* **2010**, *45*, 199.
12. Yin, Y.; Lu, Y.; Sun, Y.; Xia, Y. *Nano Lett.* **2002**, *2*, 427.
13. Kim, H. W.; Lee, J. W.; Lee, C.; Kebede, M. A. *Polym. Adv. Technol.* **2009**, *20*, 246.
14. Schroedter, A.; Weller, H.; Eritja, R.; Ford, W. E.; Wessels, J. M. *Nano Lett.* **2004**, *2*, 1363.
15. Pan, A.; Wang, S.; Liu, R.; Li, C.; Zou, B. *Small* **2005**, *1*, 1058.
16. Zhu, Y.; Bando, Y. *Chem. Phys. Lett.* **2003**, *377*, 367.
17. Mirov, S. B.; Fedorov, V. V.; Grahaw, K.; Moskalev, I. S.; Badikov, V. V.; Panyutin, V. *Opto. Lett.* **2002**, *27*, 909.
18. Zhang, X. T.; Ip, K. M.; Liu, Z.; Leung, Y. P.; Li, Q.; Hark, S. K. *Appl. Phys. Lett.* **2004**, *84*, 2641.
19. Chan, Y. F.; Duan, X. F.; Chan, S. K.; Sou, I. K.; Zhang, X. X.; Wang, N. *Appl. Phys. Lett.* **2003**, *83*, 2665.
20. Zhang, T.; Shen, Y.; Hu, W.; Sun, J.; Wu, J.; Ying, Z.; Xu, N. *J. Vac. Sci. Technol. B* **2007**, *25*, 1823.
21. Solanki, R.; Huo, J.; Freeouf, J. L. *Appl. Phys. Lett.* **2002**, *81*, 3864.
22. Jun, J.; Park, S.; Lee, J.; Lee, C. *J. Mater. Sci. : Mater. Electron.* **2009**, *20*, 1150.
23. Fanfair, D.; Korgel, B. *Chem. Mater.* **2007**, *19*, 4943.
24. Lei, Y.; Zhang, L. D.; Meng, G. W.; Li, G. H.; Zhang, X. Y.; Liang, C. H.; Chen, W.; Wang, S. X. *Appl. Phys. Lett.* **2001**, *78*, 1125.
25. Zhang, X. T.; Liu, Z.; Ip, K. M.; Leung, Y. P.; Li, Q.; Hark, S. K. *J. Appl. Phys.* **2004**, *95*, 5752.
26. Shalish, I.; Temkin, H.; Narayanamuri, V. *Phys. Rev. B* **2004**, *69*, 245401.
27. Philipose, U.; Sun, P.; Xu, T.; Ruda, H.; Yang, L.; Kavanagh, K. L. *J. Appl. Phys.* **2007**, *101*, 014326.
28. Park, S.; Jun, J.; Lee, C. *J. Kor. Phys. Soc.* **2009**, *55*, 554.
29. Ip, K. M.; Liu, Z.; Ng, C. M.; Hark, S. K. *Nanotechnol.* **2005**, *16*, 1144.
30. Liu, Z. Q.; Xie, S. S.; Sun, L. F.; Tang, D. S.; Zhou, W. Y.; Wang, C. Y.; Liu, W.; Li, Y. B.; Zou, X. P.; Wang, G. *J. Mater. Res.* **2001**, *16*, 683.
31. Wang, Y. W.; Liang, C. H.; Meng, G. W.; Peng, X. S.; Zhang, L. D. *J. Mater. Chem.* **2002**, *12*, 651.
32. Yu, D. P.; Hang, Q. L.; Ding, Y.; Zhang, H. Z.; Bai, Z. G.; Wang, J. J.; Zou, Y. H.; Qian, W.; Xiong, G. C.; Feng, S. Q. *Appl. Phys. Lett.* **1998**, *73*, 3076.
33. Ran, G. Z.; You, L. P.; Dai, L.; Liu, Y. L.; Lv, Y.; Chen, X. S.; Qin, G. G. *Chem. Phys. Lett.* **2004**, *384*, 94.
34. Weast, R. *CRC Handbook of Chemistry and Physics*; CRC Press, Inc: 1977; 58 ed.